

Optimal control of light pulse storage and retrieval

Irina Novikova,^{1,2} Alexey V. Gorshkov,³ David F. Phillips,¹ Anders S. Sørensen,⁴ Mikhail D. Lukin,³ and Ronald L. Walsworth^{1,3}

¹Harvard-Smithsonian Center for Astrophysics, Cambridge, Massachusetts 02138, USA

²Department of Physics, College of William&Mary, Williamsburg, Virginia 23185, USA

³Department of Physics, Harvard University, Cambridge, Massachusetts 02138, USA

⁴QUANTOP, Danish National Research Foundation Centre of Quantum Optics, Niels Bohr Institute, DK-2100 Copenhagen Ø, Denmark

(Dated: October 21, 2018)

We demonstrate experimentally a procedure to obtain the maximum efficiency for the storage and retrieval of light pulses in atomic media. The procedure uses time reversal to obtain optimal input signal pulse-shapes. Experimental results in warm Rb vapor are in good agreement with theoretical predictions and demonstrate a substantial improvement of efficiency. This optimization procedure is applicable to a wide range of systems.

PACS numbers: 42.50.Gy, 32.70.Jz, 42.50.Md

Mapping of quantum states between light and matter is a topic of great current interest [1, 2, 3]. One of the leading approaches to realizing this capability is the storage of light in ensembles of radiators (warm atoms, cold atoms, impurities in solids, etc.) using a dynamic form of electromagnetically induced transparency (EIT) [1, 4, 5, 6, 7, 8, 9]. This light storage technique has been shown experimentally to preserve optical phase coherence [10] as well as quantum correlations and states [11, 12]; and thus has emerged as a promising technique for applications such as single-photon generation on demand [13, 14, 15, 16, 17] and quantum memories [18, 19, 20] and repeaters [21, 22, 23]. However, practical applications will require significant improvements in the efficiency of writing, storing and retrieving an input photon state beyond values achieved to date [24, 25, 26, 27]. As an advance in this direction, we report in this Letter an experimental demonstration of an optimization protocol based on time reversal [28], which determines the input signal pulse-shape that is written, stored, and retrieved with maximum efficiency for a given set of experimental conditions. This optimization procedure should be applicable to a wide range of ensemble systems in both classical and quantum regimes.

We consider the interaction of a weak (classical or quantum) signal pulse and a strong (classical) control field with a Λ -type medium. While the optimization procedure is applicable to a wide class of regimes, we focus here on resonant light-atom interactions under EIT conditions. The group velocity of the signal pulse is proportional to the intensity of the control field, such that the quantum state of the signal pulse can be reversibly stored in a collective spin coherence (spin-wave) of the atomic ensemble by reducing the control field to zero [1]. For ideal writing, storage, and retrieval, the signal pulse's frequency components must fit well within the EIT spectral window ($\Delta\omega_{\text{EIT}}$) to avoid incoherent absorptive loss: i.e., $1/t_s \ll \Delta\omega_{\text{EIT}} \simeq \sqrt{d}v_g/L$ [6], where t_s is the temporal length of the signal pulse, v_g is the group velocity of the signal pulse inside the EIT medium at full con-

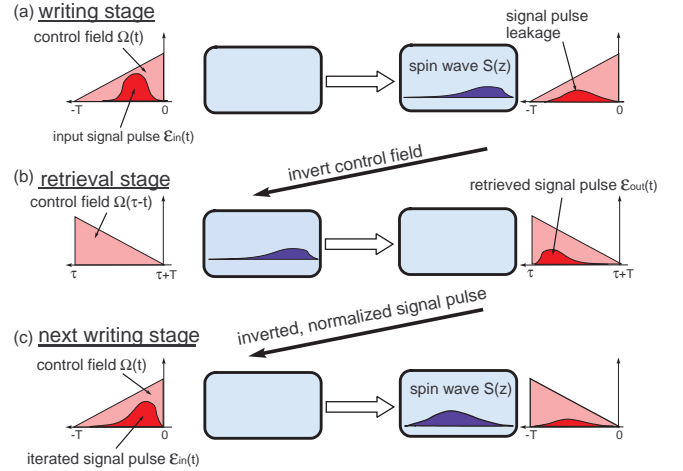


FIG. 1: (color online) Schematic of the iterative signal pulse optimization procedure described in the text. (a) An input signal pulse $\mathcal{E}_{\text{in}}(t)$ is mapped into a spin-wave $S(z)$ using a control field envelope $\Omega(t)$. (b) After a storage period τ , the spin-wave is mapped into an output signal pulse $\mathcal{E}_{\text{out}}(t)$ using the time-reversed control field envelope $\Omega(\tau - t)$. (c) The time-reversed and normalized version of the measured $\mathcal{E}_{\text{out}}(t)$ is used as the input \mathcal{E}_{in} in the next iteration.

trol field intensity, L is the length of the medium, and d is the optical depth of the medium for the signal pulse in the absence of EIT conditions [29]. In addition, v_g must be small enough for the entire signal pulse to be spatially compressed into the ensemble before storage — i.e., $v_g t_s \ll L$ — so as to avoid “leakage” of the front edge of the pulse outside the medium before the back edge has entered. Simultaneous satisfaction of both these conditions is possible only at very large optical depth d , i.e., at high density and/or large sample size. However, operation at very large d can degrade EIT performance and shorten the spin-wave coherence lifetime due to radiation trapping, competing nonlinear processes, etc. Therefore,

practical, high-efficiency light storage will likely be performed at moderately large d and require optimization of the input signal pulse-shape to minimize absorptive and leakage losses.

Recently, a procedure to determine the optimal input signal pulse-shape for a given optical depth and control field was proposed [28]. This optimization procedure is based on successive time-reversal iterations and shown schematically in Fig. 1. First, for a given input control field with Rabi frequency envelope $\Omega(t)$, a trial input signal pulse with envelope $\mathcal{E}_{\text{in}}(t)$ is mapped into a spin-wave $S(z)$ inside the atomic ensemble (writing stage). ($\mathcal{E}_{\text{in}}(t)$ and the input control field are taken to be non-zero over the time-interval $[-T, 0]$.) In general there will be some absorptive and leakage losses during this writing process. After a storage period τ , an output control field $\Omega(\tau - t)$ — i.e., the time-reversed version of the input control field — is used to map $S(z)$ back into an output signal pulse $\mathcal{E}_{\text{out}}(t)$, which leaves the medium and is measured (retrieval stage). The input signal pulse for the next iteration is then generated with a pulse-shape corresponding to a time-reversed version of the previous output signal pulse and an amplitude normalized to make the energy of the pulse equal to a fixed target value. These steps are then repeated iteratively, using the same input and output control fields, until the shape of the output signal pulse on a given iteration is identical to the time-reversed profile of its corresponding input signal pulse. The resulting signal pulse-shape is predicted to provide the highest write/store/retrieve efficiency possible for a given optical depth and control field profile, and should be applicable to both quantum and weak classical signal pulses.

In the experiment reported here, we tested this optimization procedure and confirmed its three primary predictions:

1. The write/store/retrieve efficiency (the ratio of energies carried by the retrieved and input signal pulses) grows with each iteration until the input signal field converges to an optimal pulse-shape. See Fig. 2.
2. For a given control field profile and optical depth d , the optimization procedure converges to the same input signal pulse-shape and the same maximum efficiency, independent of the initial (trial) signal pulse-shape. See Fig. 3.
3. For a given optical depth, different control field profiles result in different optimal signal pulse-shapes but yield the same maximum efficiency, provided spin-coherence decay during the writing and retrieval stages is small. See Fig. 4.

We performed these experimental demonstrations using a standard Rb vapor EIT setup, similar to that described in Ref. [30]. A cylindrical 7.5 cm-long glass cell containing isotopically enriched ^{87}Rb and 40 Torr Ne buffer gas was mounted inside a three-layer magnetic shield to reduce stray magnetic fields. The Rb vapor cell was typically operated at a temperature $\simeq 60^\circ\text{C}$, corresponding to a Rb vapor density $\simeq 2.5 \times 10^{11} \text{ cm}^{-3}$ and an optical depth $d \simeq 9.0$. Optical fields near the Rb $D1$

transition (795 nm) were used for EIT and light storage. These fields were created by phase-modulating the output of an external-cavity diode laser using an electro-optical modulator (EOM) operating at the ground state hyperfine frequency of ^{87}Rb (6.8 GHz). The laser carrier frequency was tuned to the $5^2\text{S}_{1/2}F = 2 \rightarrow 5^2\text{P}_{1/2}F' = 2$ transition and served as the control field during light storage; while the high-frequency modulation sideband, resonant with the $5^2\text{S}_{1/2}F = 1 \rightarrow 5^2\text{P}_{1/2}F' = 2$ transition, served as the signal field. The amplitudes of the control and signal fields could be changed independently by simultaneously adjusting the EOM amplitude and the total intensity in the laser beam using an acousto-optical modulator (AOM). Typical peak control field and signal pulse powers $\sim 5 \text{ mW}$ and 0.1 mW , respectively. The laser beam was collimated to a Gaussian cylindrical beam of relatively large diameter ($\simeq 7 \text{ mm}$) and then circularly polarized using a quarter-wave plate before entering the vapor cell. The Rb atom diffusion time out of the laser beam ($\simeq 7 \text{ ms}$) was long enough to have negligible effects [31]. Small, remnant magnetic fields were the leading source of spin decoherence, with typical spin-wave decay time constants $\simeq 2 \text{ ms}$. We used relatively short pulses and storage times, such that spin decoherence had a negligible effect except for a modest reduction of the efficiency of the storage process.

Fig. 2 shows an example implementation of the iterative optimization procedure, using a step-like control field and a trial input signal pulse with a Gaussian profile. Some portions of the first input pulse were incoherently absorbed or escaped the cell before the control field was turned off; but a fraction was successfully mapped into an atomic spin-wave, stored for $400 \mu\text{s}$, and then retrieved and detected. This retrieved signal pulse-shape was used to generate a time-reversed and normalized input signal pulse for the next iteration. After a few iterations, both the input and output signal pulses converged to fixed profiles, with the write/store/retrieve efficiency increasing with each iteration and reaching a maximum. In general, different trial input pulses all converged to the same optimal signal pulse-shape (e.g., see Fig. 3). In addition, systematic variation of the signal pulse-shape uniformly yielded lower efficiencies than the pulse-shape given by the optimization procedure.

We performed similar optimization experiments for a wide range of control field profiles. Some example results are shown in Fig. 4. In general we found different optimized signal pulse-shapes for different control field profiles; however, the optimized write/store/retrieve efficiency was independent of the control field profile. This observation is consistent with the theoretical prediction [28] that optimal light-storage efficiency does not depend on the control field, but only on the optical depth, provided spin decoherence and other loss mechanisms can be neglected during the writing and retrieval stages.

To compare our experimental results with theoretical calculations, we approximated the 16-level structure of the ^{87}Rb D_1 line with a single three-level Λ -system and

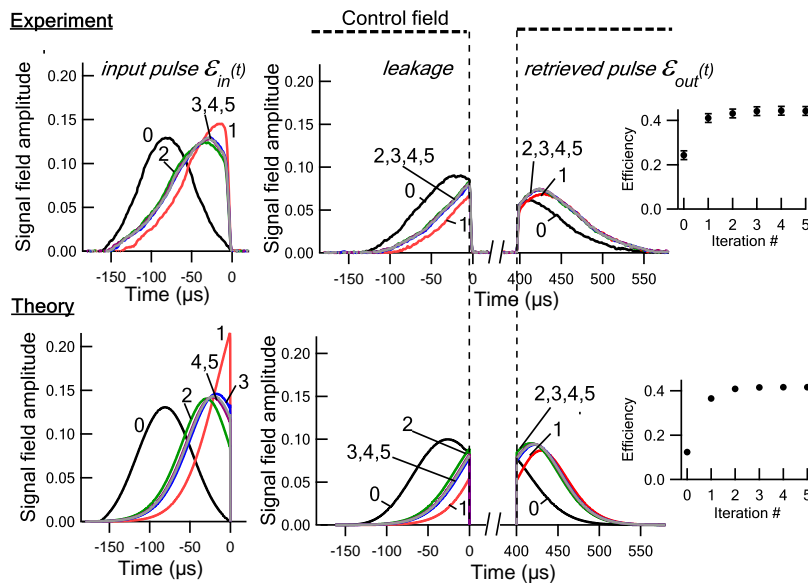


FIG. 2: (color online) Top: Example data for the signal pulse optimization procedure, using a constant control field during writing and retrieval (timing indicated by dashed lines) and a 400 μs storage interval. *Left*: input signal pulses \mathcal{E}_{in} , labeled by the iteration number and beginning with a trial Gaussian input pulse (iteration “0”). *Center*: signal pulse leakage for each iteration. *Right*: output signal pulse \mathcal{E}_{out} for each iteration. *Inset*: Write/store/retrieve efficiency determined from the measured input and output signal pulses: $\int \mathcal{E}_{out}^2 dt / \int \mathcal{E}_{in}^2 dt$. Bottom: theoretical calculation of the signal pulse optimization procedure, using the model described in the text and the experimental conditions of the measurements in the top panel. *Inset*: Calculated write/store/retrieve efficiency.

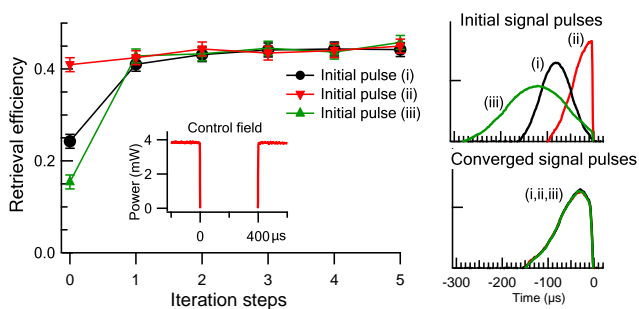


FIG. 3: (color online) Example data illustrating that the iterative optimization procedure converges to the same signal pulse-shape and maximum efficiency independent of the initial signal pulse-shape, for a given control field profile (shown in inset) and optical depth ($d=9.0$).

modeled stored light dynamics as follows [1, 6, 28]:

$$(\partial_t + c\partial_z)\mathcal{E}(z, t) = ig\sqrt{N}P(z, t), \quad (1)$$

$$\partial_t P(z, t) = -\gamma P(z, t) + ig\sqrt{N}\mathcal{E}(z, t) + i\Omega(t - z/c)S(z, t), \quad (2)$$

$$\partial_t S(z, t) = -\gamma_s S(z, t) + i\Omega(t - z/c)P(z, t) \quad (3)$$

Here \mathcal{E} is the slowly-varying envelope for the signal field, P is the transverse polarization of the atomic ensemble on the optical transition driven by the signal field, S is the spin-wave envelope, and Ω is the control field Rabi

frequency envelope. Also, $g\sqrt{N}$ is the coupling strength between the atomic ensemble and the signal field, where g is the corresponding one-photon Rabi frequency and N is the number of atoms along the laser beam that are available to participate in light storage after optical pumping by the control field; γ is the decoherence rate of P , due primarily to buffer gas collisions; and γ_s is the spin-wave decoherence rate. To calculate Ω , we used the dipole matrix element of the $|F = 2, m_F = 1\rangle \rightarrow |F' = 2, m_F = 2\rangle$ transition, which was the dominant control field transition for our experimental conditions [32]. We approximated the laser beam profile as a uniform cylindrical beam with the same diameter and total power as used in the experiment.

We solved Eqs. (1-3) analytically by adiabatically eliminating P , an excellent approximation for our experimental conditions. We then calculated the results of the iterative optimization procedure: i.e., the output signal field (both signal leakage and stored/retrieved pulses) as well as the generated input signal pulse for each successive iteration. For these calculations we used values for $g\sqrt{N}$, γ , γ_s , and the trial input signal pulse and control field appropriate for the particular experimental conditions. Example results of these calculations are shown in the bottom panels of Fig. 2. The calculated output signal pulse-shapes are qualitatively similar to the experimental results and converge to an optimal input signal pulse-shape within a few iteration steps. The calculated efficiencies for the optimization procedure, shown

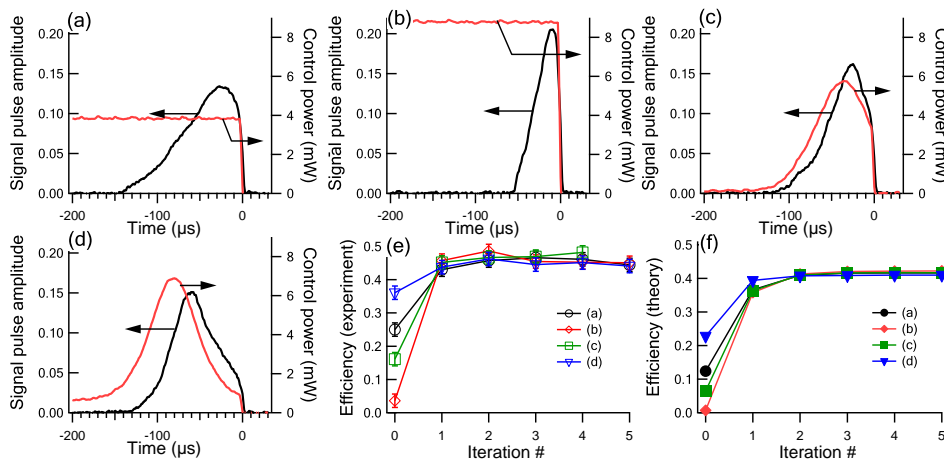


FIG. 4: (color online) (a)-(d) Examples of optimal input signal pulses determined experimentally by application of the iterative optimization procedure, for different control field profiles. In all cases, the initial (trial) signal pulse has the same Gaussian pulse-shape and amplitude as the trial pulse used in the data shown in Fig. 2. (e) Experimentally measured and (f) calculated write/store/retrieve efficiencies as functions of the iteration number.

in Figs. 2 and 4(f), are in reasonable agreement with experiment. We also confirmed that the effects of inhomogeneous Doppler broadening were small for the buffer gas pressure used in our experiments, by repeating the calculations in a more realistic approximation that included Doppler broadening of Rb atoms as well as velocity changing collisions with buffer gas atoms.

In conclusion, we experimentally demonstrated an iterative optimization procedure, based on time-reversal, to find the input signal pulse-shape that maximizes the efficiency of light storage and retrieval. We confirmed the three primary predictions of the theory underlying the optimization procedure [28]: (i) efficiency grows with each iteration until the input signal field converges to its optimal pulse-shape; (ii) the result of the optimization procedure is independent of the initial (trial) signal pulse-shape; and (iii) the optimal efficiency does not depend on the control field temporal profile. We also performed theoretical calculations of the light storage process and

the optimization procedure, and found good qualitative agreement with the experimental results, thus supporting the interpretation that optical depth is the key figure of merit for light storage efficiency. The optimization procedure should be applicable to both classical and quantum signal pulses and to a wide range of ensemble systems. As one example, since pulse-shape optimization with weak classical light pulses can be straightforwardly performed, such optimization could be used to determine the temporal profile of input quantum fields, for which mode-shape generation and measurement are much more difficult to carry out. Also, pulse-shape optimization of the kind demonstrated here in atomic ensembles could be applicable to other systems, *e.g.*, photonic crystals [33].

We are grateful to M. Hohensee for useful discussions, and to M. Klein and Y. Xiao for assistance in experiments. This work was supported by ONR, DARPA, NSF, Danish Natural Science Research Council, Packard foundation, and the Smithsonian Institution.

-
- [1] M. D. Lukin, *Rev. Mod. Phys.* **75**, 457 (2003).
[2] B. Julsgaard *et al.*, *Nature* **432**, 482 (2004).
[3] B. Kraus *et al.*, *Phys. Rev. A* **73**, 020302 (2006).
[4] S. E. Harris, *Phys. Today* **50**(7), 36 (1997).
[5] M. Fleischhauer, A. Imamoglu, and J. P. Marangos, *Rev. Mod. Phys.* **77**, 633 (2005).
[6] M. Fleischhauer and M. D. Lukin, *Phys. Rev. Lett.* **84**, 5094, (2000); *Phys. Rev. A* **65**, 022314 (2002).
[7] C. Liu, Z. Dutton, C. H. Behroozi, and L. V. Hau, *Nature* **409**, 490 (2001).
[8] D. F. Phillips *et al.*, *Phys. Rev. Lett.* **86**, 783 (2001).
[9] P. R. Hemmer *et al.*, *Opt. Lett.* **26**, 361 (2001); J. J. Longdell *et al.*, *Phys. Rev. Lett.* **95**, 063601 (2005).
[10] A. Mair *et al.*, *Phys. Rev. A* **65**, 031802(R) (2002).
[11] A. Kuzmich *et al.*, *Nature* **423**, 731 (2003).
[12] C. H. van der Wal *et al.*, *Science* **301**, 196 (2003).
[13] C. W. Chou, S. V. Polyakov, A. Kuzmich, and H. J. Kimble, *Phys. Rev. Lett.* **92**, 213601 (2004).
[14] D. N. Matsukevich and A. Kuzmich, *Science* **306**, 663 (2004).
[15] M. D. Eisaman *et al.*, *Phys. Rev. Lett.* **93**, 233602 (2004).
[16] D. N. Matsukevich *et al.*, *Phys. Rev. Lett.* **97**, 013601 (2006).
[17] S. Chen *et al.*, *Phys. Rev. Lett.* **97**, 173004 (2006).
[18] C. W. Chou *et al.*, *Nature* **438**, 828 (2005).
[19] T. Chanelière *et al.*, *Nature* **438**, 833 (2005).
[20] M. D. Eisaman *et al.*, *Nature* **438**, 837 (2005).
[21] L. M. Duan, M. D. Lukin, J. I. Cirac, and P. Zoller,

- Nature **414**, 413 (2001).
- [22] T. Chanelière *et al.*, Phys. Rev. Lett. **96**, 093604 (2006).
- [23] D. Felinto *et al.*, Nature Phys. **2**, 844 (2006).
- [24] I. Novikova, M. Klein, D. F. Phillips, and R. L. Walsworth, Proc. SPIE. **5735**, 87 (2005).
- [25] D. Felinto *et al.*, Phys. Rev. A **72**, 053809 (2005).
- [26] J. Laurat *et al.*, Opt. Expr. **14**, 6912 (2006).
- [27] J. K. Thompson, J. Simon, H. Loh, and V. Vuletić, Science **313**, 74 (2006).
- [28] A. V. Gorshkov *et al.*, quant-ph/0604037 (2006); quant-ph/0612082; quant-ph/0612083; quant-ph/0612084.
- [29] We define the optical depth d as describing $1/e$ amplitude attenuation of a weak resonant signal pulse with no control field.
- [30] I. Novikova, Y. Xiao, D. F. Phillips, and R. L. Walsworth, J. Mod. Opt. **52**, 2381 (2005).
- [31] Y. Xiao, I. Novikova, D. F. Phillips, and R. L. Walsworth, Phys. Rev. Lett. **96**, 043601 (2006).
- [32] As in Refs. [6, 28], we define the Rabi frequency Ω as $|\Omega|^2 = \wp^2 I / (2\hbar^2 \epsilon_0 c)$, where \wp is the transition dipole matrix element and I is the control field intensity.
- [33] M.F. Yanik, *et. al.*, Phys. Rev. Lett. **93**, 233903 (2004).